AGU PUBLICATIONS

Water Resources Research

TECHNICAL REPORTS: DATA

10.1002/2016WR019261

Key Points:

- Half-hourly discharge and water temperature for 2002–2015 in 6 subbasins, Tuolumne River, CA
- Daily inflow of the Tuolumne River to the Hetch Hetchy Reservoir for 1970-2015
- Meteorological and snow data are provided

Supporting Information:

- Supporting Information S1

Correspondence to:
J. D. Lundquist,
jdlund@u.washington.edu

Citation:
Lundquist, J. D., et al. (2016), Yosemite Hydroclimate Network: Distributed stream and atmospheric data for the Tuolumne River watershed and surroundings, *Water Resour. Res.*, *52*, doi:10.1002/2016WR019261.

Received 25 MAY 2016
Accepted 1 SEP 2016
Accepted article online 6 SEP 2016

Yosemite Hydroclimate Network: Distributed stream and atmospheric data for the Tuolumne River watershed and surroundings

Jessica D. Lundquist[1], James W. Roche[2], Harrison Forrester[2], Courtney Moore[3], Eric Keenan[1], Gwyneth Perry[1], Nicoleta Cristea[1], Brian Henn[1], Karl Lapo[1], Bruce McGurk[4], Daniel R. Cayan[5,6], and Michael D. Dettinger[6]

[1]Department of Civil and Environmental Engineering, University of Washington, Seattle, Washington, USA, [2]National Park Service, Yosemite, California, USA, [3]Northwest Hydraulic Consultants, Seattle, Washington, USA, [4]McGurk Hydrologic, Orinda, California, USA, [5]Scripps Institution of Oceanography, La Jolla, California, USA, [6]United States Geological Survey, Reno, Nevada

Abstract Regions of complex topography and remote wilderness terrain have spatially varying patterns of temperature and streamflow, but due to inherent difficulties of access, are often very poorly sampled. Here we present a data set of distributed stream stage, streamflow, stream temperature, barometric pressure, and air temperature from the Tuolumne River Watershed in Yosemite National Park, Sierra Nevada, California, USA, for water years 2002–2015, as well as a quality-controlled hourly meteorological forcing time series for use in hydrologic modeling. We also provide snow data and daily inflow to the Hetch Hetchy Reservoir for 1970–2015. This paper describes data collected using low-visibility and low-impact installations for wilderness locations and can be used alone or as a critical supplement to ancillary data sets collected by cooperating agencies, referenced herein. This data set provides a unique opportunity to understand spatial patterns and scaling of hydroclimatic processes in complex terrain and can be used to evaluate downscaling techniques or distributed modeling. The paper also provides an example methodology and lessons learned in conducting hydroclimatic monitoring in remote wilderness.

1. Introduction

Mountains are the water towers of the world, with high elevations and complex topography in often protected, wilderness locations. These regions are critical to understand scientifically and yet challenging to observe and monitor [e.g., *Burt and McDonnell*, 2015]. Here we provide a set of distributed measurements of streamflow, water temperature, and atmospheric variables spanning a period of over 10 years in the Tuolumne River Watershed, Yosemite National Park, Sierra Nevada, California, USA. These data could be used for distributed hydrologic modeling, for evaluation of remote sensing products, or for testing atmospheric downscaling techniques. Lessons learned from the Tuolumne network can provide an example of how to establish a similar network in another mountain location.

1.1. Basin Overview

The upper Tuolumne River Watershed was made famous by John Muir's "first summer in the Sierra" in 1870 [*Muir*, 1911] and became protected as part of Yosemite National Park in 1890. The summer headquarters of the Sierra Club from 1912 to 1973 were located in Tuolumne Meadows beside the river [*O'Neill*, 1984], and the watershed drains to the Hetch Hetchy Reservoir behind the O'Shaughnessy Dam, which was initially constructed in 1923, completed in 1938, and provides hydropower and drinking water to the city of San Francisco and other cities on the San Francisco peninsula. The study area encompasses more high elevations (focus area from 2600 to 4000 m) and covers a larger total area (over 1000 km^2) than most research basins in the western USA, e.g., Reynolds Creek [*Reba et al.*, 2011]; the Southern Sierra Critical Zone Observatory [*Hartsough and Meadows*, 2012]; Kings River Experimental Watersheds [*Hunsaker et al.*, 2012]; or Senator Beck [*Landry et al.*, 2014]. The location provides both opportunities and challenges. The Tioga Road (California Highway 120), the highest pass over the Sierra Nevada at over 3000 m, provides road access during the summer months only, and many wilderness sites are accessible only by foot. The natural granitic bedrock of

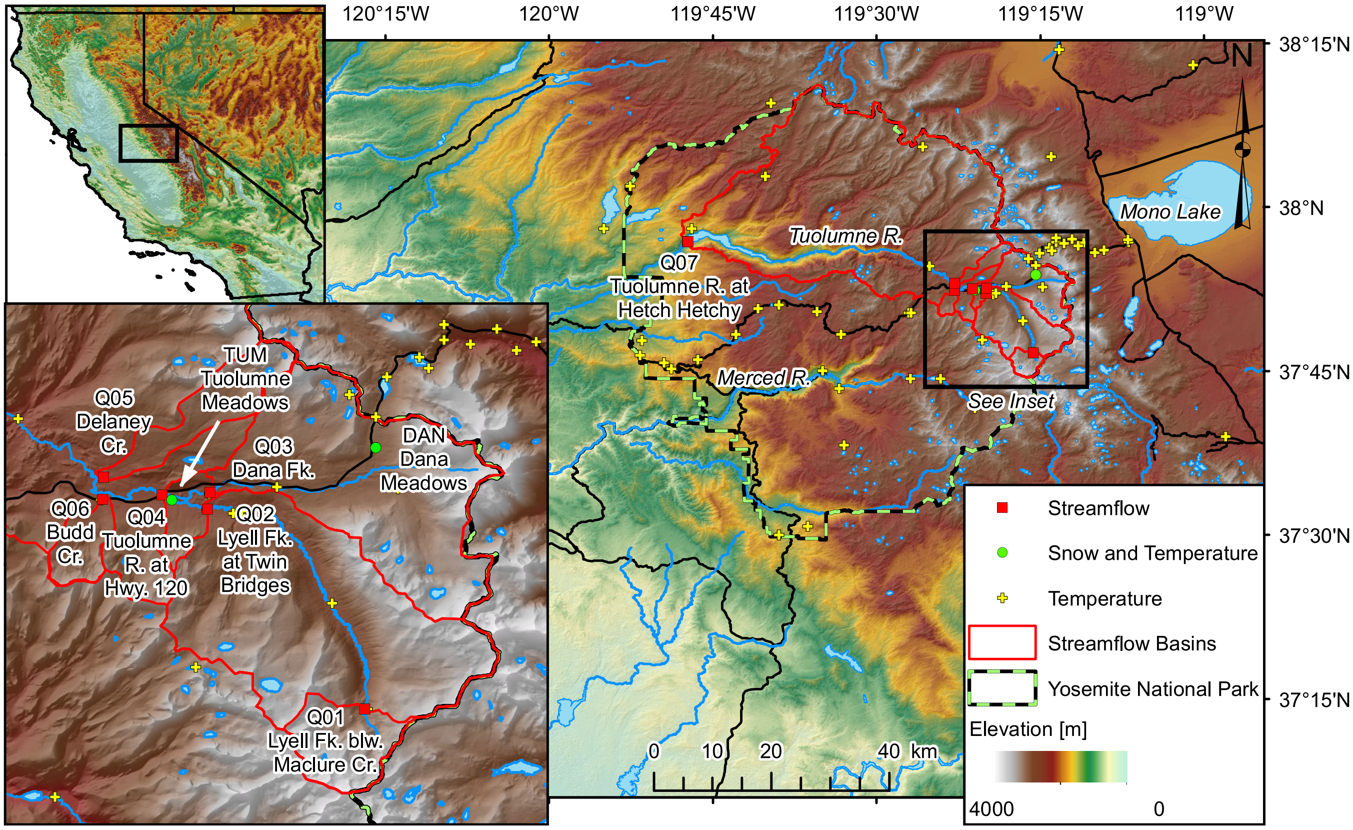

Figure 1. Map of all data sites included in this paper. The yellow crosses are temperature sensor locations. The red squares are streamflow sites included in this archive. The green dots are locations of snow stations, which were also used to create the meteorological forcing data set (with precipitation only taken from the Tuolumne site and all other values taken from the Dana Meadows site).

the region provides well-controlled, stable stream channels in many locations. The wilderness setting preserves the natural characteristics of the drainage but also requires unique installation practices in order to comply with wilderness regulations, which are detailed further below.

The Tuolumne River drainage is fairly typical of the central to southern Sierra Nevada, with its high and cold drainages, winter-precipitation-dominated climate, steep terrain, rapid snowmelt seasons, and relatively thin soils. The area contributing to the Tuolumne River as it enters Tuolumne Meadows is about 186 km^2, and the area contributing to Hetch Hetchy Reservoir is about 1181 km^2 (Figure 1). The Tioga glaciation (about 30,000–15,000 years ago) removed most sedimentary material, leaving broad U-shaped valleys, polished domes, and steep headwater cirques [*Huber*, 1987]. Today two relatively small glaciers, Lyell and Maclure, contribute to the Lyell Fork of the Tuolumne and remain as remnants from the Little Ice Age about 250 years ago [*Basagic and Fountain*, 2011]. Approximately 90% of the drainage is underlain by intrusive rocks (chiefly granodiorite; National Park Service (NPS) records of test well drilling), which erode slowly and interact little with the streamflow [*Huber*, 1987]. The underlying granodiorite bedrock in the basin allows us to assume minimal losses to the deep groundwater system, which is a major source of uncertainty in hydrologic observations and modeling in many other locations. The highest third of the Dana Fork subbasin is underlain by metavolcanic and metasedimentary rock, which tends to be more highly fractured than granodiorite and may result in more subsurface flow than other basin areas. Soil depths are typically 1 m or less, with maximum recorded depths of 3–5 m in flat meadow locations [*Lowry et al.*, 2011], which is consistent with reported values [*Natural Resources Conservation Service*, 2006]. Precipitation falls primarily as snow (>90% snow for the watershed above the Tuolumne River at Highway 120 in most years), with normal annual peak stream discharge typically occurring in May or June due to snowmelt. Approximately 50% of the drainage area above the Tuolumne River at Highway 120 lies between 2800 and 3300 m elevation, with 25% above and 25% below this range. The data set here includes stream stage, water temperature, and discharge at half-hourly time steps for water years 2002–2015 from six subbasins contributing to this watershed, as well as hourly point and daily distributed meteorological and snow water equivalent (SWE) data (Figure 1 and Table 1). We also include daily inflows calculated from the water balance at Hetch Hetchy Reservoir.

1.2. History of the Yosemite Hydroclimate Monitoring Network and Unique Research Results to Date

In summer 2001, a group of researchers from Scripps Institution of Oceanography decided to be "high-altitude oceanographers" and began installing pressure transducers in the area's streams and temperature sensors in the area's trees. The goal was threefold—to better understand fine-scale variation in hydroclimatic variables at high elevations [*Lundquist et al*., 2003], to understand how diurnal cycles in streamflow varied through a watershed system [*Lundquist*, 2004; *Lundquist et al*., 2005], and to explore the extent to which deployment of numerous, new, and inexpensive monitoring instruments—in tandem with a few traditional high-quality measurement stations—might support greater overall hydrometeorological data coverage in a complex terrain [*Bales et al*., 2006]. Gauge locations were chosen to sample basins with varying elevation ranges, slopes, and aspects, while also considering practicalities, such as access. The most distant site from the road (Lyell Fork below Maclure) samples the basin headwaters immediately downstream of the two glaciers, which are a critical source of water in late summer.

With the exception of sites adjacent to the road, the entire study area is in federally designated wilderness, where any instrument installations must comply with the Wilderness Act of 1964 (Public Law 88-577) and the National Environmental Policy Act (NEPA) of 1970 (Public Law 91-190). These laws require that installations have the minimum possible impact to the environment, including minimal visibility to wilderness visitors. For this reason, weirs, which are typical in other research catchments, were not used. Instead, installations were designed to be nearly invisible to park visitors desiring a wilderness experience, while still meeting research and operational needs for high data quality, such as providing the Park with essential information for management of floods, water withdrawals, and long-term change [*Lundquist and Roche*, 2009]. All sites were developed in close partnership between university researchers, the United States Geological Survey (USGS), and the NPS.

Initial years of stream stage data revealed patterns in the timing of how water travels through a snow-fed mountain system. Sometimes a rapid temperature increase causes the onset of spring melt to occur simultaneously across all elevations [*Lundquist et al*., 2004], although when a similar increase occurs earlier in the year, melt is delayed in north-facing basins because the sun is lower in the sky [*Lundquist and Flint*, 2006]. Diurnal cycles in streamflow occur in all of these basins, but the hourly timing of peak flow is controlled by different processes in basins of different sizes [*Lundquist and Dettinger*, 2005; *Lundquist et al*., 2005]. Distributed air temperature data demonstrated how mountain temperatures often do not vary linearly with elevation but still have topographically predictable spatial patterns [*Lundquist and Cayan*, 2007; *Lundquist et al*., 2008]. Similarly, patterns of relative humidity (dewpoint temperature) are more complex than those typically represented in empirical equations based on elevation, but can be well captured by high-resolution atmospheric models [*Feld et al*., 2013]. As years went on, rating curves were developed, and estimated discharge values were used as boundary conditions for simulations of groundwater levels in Tuolumne Meadows [*Lowry et al*., 2010, 2011] and for hydrologic model evaluation [*Cristea et al*., 2014; *Hinkelman et al*., 2015] and precipitation evaluation [*Henn et al*., 2015].

The stream network led to new real-time monitoring sites within the basin. Beginning in water year 2007, the City and County of San Francisco Public Utilities sponsored installation of an official USGS streamflow gaging station in the Tuolumne River just above its inflow to the Hetch Hetchy Reservoir (measuring stage, discharge, water temperature, turbidity and conductivity, and accessible in real-time as USGS gauge #11274790 at waterdata.usgs.gov). Falls Creek, which drains to the Hetchy Hetchy Reservoir from the north, has historic USGS discharge data (water years 1916–1983, USGS gauge #11275000) and was reinitialized in 2009 as the FHH site in the cdec.water.ca.gov data system. More recently (in water year 2014), another real-time station, corresponding to the Tuolumne River at Highway 120 site provided here, was established with stage measurements and discharge estimates available at the TUM site in the cdec.water. ca.gov data system. Potential users of these data are advised that the rating curves used in the cdec.water. ca.gov system may not be up to date.

Due to its high elevation and greater-than-average extent of meadows, the Tuolumne River basin has also been a focus of many snow remote sensing studies, including evaluations of snow cover extent [*Rice et al*.,

Table 1. List of Sites, Locations, and Data Availability, all Geographic Coordinates use NAD 83 Datum[a]

Site Code	Site Name	Latitude (°)	Longitude (°)	Basin Area (km^2)	Elevation (m)	Water Years With Data (X = Data Available)														Data Time Step (h)	Raw Data Available	Quality	Type of Installation
						02	03	04	05	06	07	08	09	10	11	12	13	14	15				
Q01	Lyell below Maclure	37.777	−119.261	15	2940				X	X	X		X	X	X	X	X	X	X	0.5	Yes	B	Solinst, Stilling tube
																	X	X	X				Vented Transducer
Q02a	Lyell Fork at Twin Bridges, upstream	37.869	−119.331	109	2640					X	X	X	X	X	X	X	X	X	X	0.5	Yes	A	Solinst, Stilling tube; Vented transducer installed 16 Jul 2015
Q02b	Lyell Fork at Twin Bridges, downstream	37.869	−119.331	109	2640	X	X	X	X	X	X	X		X	X					0.5	Yes	B	Solinst, anchor
Q03a	Dana Fork, lodge	37.876	−119.333	74	2650	X	X	X	X	X										0.5	Yes	C	Solinst, anchor
Q03b	Dana Fork, Bug Camp	37.877	−119.338	75	2640					X	X	X	X	X	X	X	X	X	X	0.5	Yes	A	Solinst, Stilling tube; Vented transducer (12 Jun 2015 to present)
Q04	Tuolumne 120	37.876	−119.355	186	2600	X	X	X	X											0.5	Yes	A	Solinst, anchor
										X	X		X	X	X	X	X	X	X				Solinst, Stilling tube
																	X	X	X				Vented Transducer installed Oct 2012.
Q05	Delaney Creek, meadow	37.883	−119.381	16	2600							X	X	X	X	X	X	X	X	0.5	Yes	B	Solinst, Stilling tube
Q06a	Budd Creek upstream	37.873	−119.382	7	2600						X	X	X	X	X		X	X	X	0.5	Yes	C	Solinst, Stilling tube
Q06b	Budd Creek downstream	37.874	−119.382			X	X	X	X	X			X			X	X	X	X	0.5	Yes	C	Solinst, anchor
Q07	Hetch Hetchy Reservoir	37.9708	−119.7883	1181	1162	X	X	X	X	X	X	X	X	X	X	X	X	X	X	24	No	A	See text
TUM	Tuolumne Snow Pillow and Precip	37.8730	−119.3500	NA	2600	X	X	X	X	X	X	X	X	X	X	X	X	X	X	1	No		Precipitation**
						X	X	X	X	X	X	X	X	X		X			X	24			SWE (pillow)
						X	X	X	X	X	X	X	X	X	X	X	X	X	X	Available approximately monthly in the spring			SWE (snow course)
DAN	Dana Snow Pillow and Met	37.896	−119.257	NA	3000	X	X	X	X	X	X	X	X	X	X	X	X	X	X	1	No		Tair, RH, wind, incoming shortwave
						X	X	X	X	X				X	X	X	X	X	X	24	No		SWE (pillow)
						X	X	X	X	X	X	X	X	X	X	X	X	X	X	Available approximately monthly in the spring			SWE (snow course)
	Distributed T_{mean}, T_{min}, T_{max}	62 sites, see metadata				X	X	X	X											24	No		Air temperature

[a]Order of stream sites matches supporting information, from upstream to downstream. Although 95% confidence intervals are provided for discharge at all sites except Budd Creek and Hetch Hetchy, we provide here a qualitative rating of the relative quality of the discharge data at each site, where A = our best sites; B = intermediate-quality sites; C = our poorest sites. **Tuolumne precipitation is provided at an hourly time step along with the meteorological data at the Dana station. The provided data are scaled to the Dana location as documented in the text and metadata files.

2011; *Raleigh et al*., 2013] and snow water equivalent reconstruction [*Rittger et al*., 2016]. From water years 2013 to present, the watershed has been a focus of the NASA Airborne Snow Observatory Campaign to use LiDAR to map snow depth at high resolution to aid in forecasting inflow to the Hetch Hetchy Reservoir [*Painter et al*., 2016] and was included in pilot flights of the HyspIRI suite of instruments (http://hyspiri.jpl.nasa.gov/airborne).

1.3. Outline of This Paper

Here we describe an archived and publicly available data set for six stream locations, 1 reservoir, 2 snow pillow and meteorology stations, and 62 air temperature locations in the vicinity of the upper Tuolumne River Watershed. Section 2 details the measurement methods and quality control applied, and section 3 discusses applications of the data. Section 4 offers conclusions.

2. Data Sets

2.1. Flow into Hetch Hetchy Reservoir

Full natural flows into the Hetch Hetchy Reservoir were determined on a daily basis through a mass balance equation that accounted for releases to the downstream reach, spills, drafts for power generation and water supply, and daily reservoir elevations that allowed for the determination of changes in storage for water years 1970–2015. Due to the cold water, relatively cool air temperature, and modest surface area of the reservoir, evaporation was not estimated. Contributions to groundwater are believed to be negligible due to the monolithic granite formations underlying the reservoir. The resultant time series was compared to the unimpaired record from the Merced River at Happy Isles Bridge near Yosemite, CA (USGS gauge #11264500) for the 1970 through 2006 period. Starting in 2007, the gauge at the upper end of the reservoir was used for the comparison (Tuolumne R at Grand Canyon of Tuolumne above Hetch Hetchy, USGS gauge #11274790). The uncertainties associated with reconstructed flows are considered to be similar to those of standard streamflow observations ($\sim\pm$10%).

2.2. Stream Stage

Aside from the reservoir, the basis for each record is a pressure transducer anchored to the bottom of the stream channel by either a concrete form or a wilderness stilling tube (see supporting information here and/or in *Lundquist et al*. [2009]). Data processing included the following: (1) remove data from times when instruments were not in the water; (2) link time series data measured by different instruments at the same location (many instruments were swapped with a new self-recording instrument each summer); (3) subtract barometric pressure to obtain a time series of water level; (4) use manual stage measurements to adjust the water level time series to correct for instrument relocation or drift; and (5) remove obviously erroneous measurements due to instrument malfunction. The stage obtained from anchored pressure transducers is less reliable than that for stilling tubes because these anchors were sometimes moved by the river at high flow and by field personnel when instruments were replaced. Care was taken to correct for these movements by adding appropriate offsets to the original time series, but depending on the availability of manual observations for quality control checks, some errors may remain. The supporting information and site metadata files included with the data set detail when and where this may be an issue.

During recent years, some sites were monitored with a vented pressure transducer in a stilling tube. These pressure sensors have a tube exposing them to atmospheric pressure as well as total stream pressure and do not require separate processing to remove atmospheric pressure, leading to smaller observational uncertainty. Table 2 details the various instruments and installation types, and quantifies expected measurement uncertainties. Although the early measurement system (a pressure sensor in a concrete anchor) was the easiest to install and had the minimal visual impact to the park wilderness, the improved data accuracy from the stilling tube and vented pressure transducer systems more than compensates for the extra installation footprint and effort ($\sim$2% error in discharge from this method compared to $\sim$15% error, see Table 2).

2.3. Stream Discharge

Manual discharge observations were taken during the months of May–September each year. Most measurements were made by wading with an AA or pygmy meter (following methods of *Rantz et al*. [1982a]), although acoustic Doppler sonar [*Oberg and Mueller*, 2007], dye-dilution [*Rantz et al*., 1982b, chap 7], and salt-dilution [*Moore*, 2004a,2004b; *Hudson and Fraser*, 2005] methods were also used at high flows.

Table 2. Stream Sensor Instrument Installations: Types and Accuracy

Installation Type	Anchored Solinst[a]	Solinst in Stilling Tube	Vented Pressure Transducer	Barometric Pressure
Description	Instrument in a PVC pipe inside a concrete anchor, which is cabled to a tree, bridge, or culvert	Instrument in PVC pipe inserted in vertical pipe attached to the streambed and bank with rebar; with cord for downloading instrument	Same as stilling tube but with data cord connected to a data logger box (typically hidden in a tree) and another cord open to the atmosphere	Instrument in a building or in a tree or in a dry groundwater well
Instrument Used	Solinst Levelogger	Solinst Levelogger	Druck[1] Or Campbell Scientific CS450 PT[2]	Solinst Barologger
Instrument Specs/Accuracy	Levelogger Model 3001: 0.1°C temp accuracy, ±0.5 cm pressure/depth accuracy; temperature compensated over the range of −10 to 40°C; drift of 0.1% of the full range (±0.5 cm for a 5 m model, used here)	Levelogger Edge and Gold: Temp accuracy ±0.05°C Pressure ±0.05% of FS (for 5 m model, this would be ±0.25 cm); Manufacturer states clock accurate to 1 minute per year, but 20 min of drift per year was typically observed in practice	Druck: 0–5 PSI Range, 0.25% accuracy; CS450: 0–7.25 PSI Range, 0.1% accuracy	Edge: ±0.05 kPa, with temperature compensation, temperature accuracy ±0.05°C
				Gold: 0.01 cm and ±0.05°C (also has temp compensation); Model 3001 same as 5 m Levelogger
Processing steps required	(1) subtract off atmospheric pressure; (2) correct for offsets in instrument location; (3) check for instrument drift; (4) develop rating curve	1, 3, and 4	3 and 4	3, and (5) adjust for temperature dependencies
Total error estimates in stage (Note that these are worst case scenarios—errors for most sites are believed to be less.)	Up to ±3 to 4 cm, with ±2 cm due to summed instrument accuracy and drift for both stream and barometric instruments; and ±1 to 2 cm more due to uncertainty in instrument location	Up to ±2 cm due to summed instrument accuracy and potential drift for both stream and barometric instruments	Up to ±0.5 cm due to summed instrument accuracy and potential drift	Up to ±1 cm due to summed instrument accuracy and potential drift
Error propagation into estimated discharge (using Lyell Fork above Twin Bridges at 0.7 m, typical summer flow, as an example)	±0.92 $m^3 s^{-1}$ to ±1.24 $m^3 s^{-1}$ (14–19%)	±0.61 $m^3 s^{-1}$ (9%)	±0.15 $m^3 s^{-1}$ (2%)	±0.30 $m^3 s^{-1}$ (5%)
Pros	Easy installation, lowest visible impact	Low visible impact; stable location and datum	Stable location and datum; lowest processing time required (saves ~8 hours of desk work per year); can reference instrument stage to field datum at each visit	
Cons	Instrument location moves through time; Most processing time required (~8 h of desk work per year per site by trained person + ~2 weeks additional time training for new person)	Error increases with atmospheric adjustment; hard to reference instrument reading to field datum while in the field	More work required to reduce visible impact (e.g., hiding conduit and annual battery swap from a hidden battery enclosure); higher instrument cost	

[a]Note that the Levelogger Gold reports water level equivalent above the datalogger's pressure zero point of 950 cm (the Edge models do not have such an offset). [1]Druck was used at Delaney Cr above PCT from 2012 to 2015; [2]Campbell Scientific CS450 was used at Lyell below Maclure 2012–present; Tuolumne at 120 2012–present; Dana at Bug Camp 2014–present; Lyell above Twin Bridges 2015–present.

Methodologies were tested by taking repeat measurements within the same hour at the same location. During these tests, measurements fell within 5–10% of each other, which can be considered the accuracy of an individual manual discharge measurement reported here.

Rating curves were developed to relate stage to discharge for each stream, and best estimates of 95% confidence intervals are provided. Where channel geometry information was available, we combined hydraulic information with stage and discharge measurements following the methodology of *LeCoz et al.* [2014]. This approach was chosen because it allows a more physically based estimation of discharge at flows higher or lower than the range of manual measurements and explicitly estimates the uncertainty of the rating curve at each stage level given the available information.

The *LeCoz et al*. [2014] method begins by using the hydraulics of the study site to determine a range of meaningful values for the unknowns in the equation:

$$Q=a(h-b)^{c} \tag{1}$$

For example, the Manning-Strickler equation ($c \sim 1.67$) can be applied to steady state, uniform flows in a rectangular channel, and the rectangular weir equation ($c \sim 1.5$) can be applied at low flows with a downstream section control. Thus, site surveys and hydraulics were used to create a first guess (Bayesian priors) for the rating curve, and then the manual discharge measurements, with their associated uncertainty (10%), were used in a Bayesian Markov-chain Monte-Carlo framework to update those rating curves to determine the best fit curve and the associated 95% uncertainty (see details in *LeCoz et al*. [2014] and in the supporting information). The methodology was used to determine the best fit break point between water levels where the rating curve became subject to a downstream section control, and different equations were used for discharge within the two ranges. In cases where water entered the flood plain at high flows, a third equation was added (see supporting information). Rating curves and associated uncertainty from this methodology were compared with a single rating curve equation and confidence bounds determined by a log-transform least squares fit to the manual stage-discharge observations (see supporting information). The best fit curve for the two methodologies was very similar at all stations, but the 95%-confidence intervals for the least squares methodology were, in general, much tighter at low flows and wider at high flows than the corresponding 95%-confidence intervals determined from the Bayesian methodology. We report the Bayesian confidence intervals in the data set because they more realistically represent low-flow uncertainty, which is critical to represent fairly since low flows are important to many park management decisions (e.g., when the Tuolumne campground or lodge would need to be closed due to a shortage of water supply for drinking and sanitation).

Due to the seasonal timing of manual measurements, which were taken between May and September, we are most confident of the calculated streamflow values during the summer [*Moore et al*., 2014]. Both higher and lower flows are associated with lower confidence. Users are advised that due to the limited access and lack of control structures, uncertainties are larger than one would expect at a typical USGS gauge station (see discussion of errors associated with shorter-term gauges in *Birgand et al*. [2013], but the 95% confidence intervals are provided to help indicate this uncertainty). All site surveys and manual measurements are provided so that users may examine and/or recalculate the rating curves or conduct additional uncertainty analysis [e.g., *Coxon et al*., 2015].

Data recorded during periods with suspected ice jams (see supporting information) were removed from the composite discharge time series (with all six stream sites in one file) but due to the subjective nature of ice jam identification, were not removed from the individual stream site data files.

2.4. Stream Temperature

Each of the stream instruments recorded half-hourly water temperature. These measurements are provided as is with the detailed stream data. Note that when and where the stream went dry, the instrument would have recorded air temperature.

2.5. Barometric Pressure

Because most of the stream instruments record absolute pressure, which is the weight of both the water and the atmosphere above them, a network of barometric pressure records were used to remove the effects of atmospheric pressure fluctuations (see supporting information and metadata). Pressure transducers are sensitive to instrument temperature fluctuations, and this is not always well-compensated for in instrument software [*Freeman et al*., 2004]. Therefore, care was taken to minimize this effect (see supporting information and metadata).

2.6. Standard Meteorological Forcing Data

Hourly temperature, relative humidity, incoming shortwave irradiance, and wind speed data for water years 2003–2015 were derived from data collected primarily at the California Department of Water Resources (CA DWR) snow pillow site at Dana Meadows (DAN; Figure 1 and see supporting information). The time series provided is a continuous record, as would be required to drive a hydrologic model. As such, it is our best estimate of the meteorology at this site based on a combination of measurements, gap-filling, and empirical estimates. Shortwave irradiance was corrected for local shading and for snow accumulating on the radiometer dome following the methodology of *Lapo et al*. [2015]. Short data gaps (<2 days in length) were filled with shortwave interpolation (see acknowledgments for link to code), while longer gaps were filled by estimating shortwave according to the methods detailed in *Bohn et al*. [2013]. Daily accumulated precipitation was measured with a weighing gauge at the Tuolumne Meadows snow pillow site. Based on the Parameter Regression against Independent Slopes Model (PRISM) [*Daly et al*., 2008], Dana Meadows (Figure 1) typically received 1.3 times the amount of precipitation as Tuolumne Meadows, and this ratio was verified by comparing snow accumulation rates at the two sites [*Cristea et al*., 2013]. In order to provide meteorological forcing representative of a single site, as is required for many hydrologic models, the Dana precipitation was estimated using this multiplier. Daily precipitation was assumed to occur uniformly over all hours of the day. Longwave irradiance was not measured. However, an estimate of incoming longwave is provided, using the *Prata* [1996] and *Deardorff* [1978] algorithms, as recommended in *Bohn et al*. [2013]. Due to the lack of direct observations, we were unable to assess the accuracy of these longwave estimates at this high altitude location.

2.7. Snow Measurements

SWE data were collected by the CA DWR snow surveys program. For the two sites mentioned above, DAN and TUM, we include manual snow course data for water years 1970–2015 and automated snow pillow data for water years 1980–2015. Snow course data are available approximately monthly from January to May, and snow pillow data are available daily. Years when a tree was growing in the middle of the Dana Meadows snow pillow were excluded from the data series [*Lundquist et al*., 2015].

2.8. Distributed Temperature and Relative Humidity

The above-referenced standard meteorological data records have been augmented in the upper Tuolumne drainage and the nearby upper Merced River drainage with widespread deployment and operation of small, inexpensive temperature, and humidity sensors. Daily mean, minimum, and maximum temperature data from the 62 stations used in *Lundquist and Cayan* [2007] are provided for the time period from 31 December 2000 to 1 February 2005, with the majority of sensors operating for water years 2002–2005. This quality-controlled data set includes data from Onset HOBO and tidbit loggers placed in evergreen trees, as well as data from area snow pillow stations, coop stations, and RAWS stations, with instrument and site specifications detailed in *Lundquist and Cayan* [2007, their Table 1 and Figure 1; also see supporting information]. While evergreen trees provide good shading from solar radiation in general [*Lundquist and Huggett*, 2008], some of the HOBO and tidbit loggers were in solitary trees, which resulted in sunlight striking them at a specific angle and resulted in some unrealistic maximum temperatures. Mean and minimum temperatures were estimated to be accurate to within 1°C. Missing data were not patched, but an analysis of how to best do so is provided in *Henn et al*. [2013]. Raw data are available for many locations at half-hourly time steps and for a longer period of record (2001–2015) but have not been quality controlled and thus are not included here.

Daily mean temperature and relative humidity data from 1 October 2002 to 30 September 2005 for the HOBO sites and snow pillow sites mentioned above are provided in the supporting information associated with *Feld et al*. [2013]. As with the temperature data, raw data from the HOBO stations are available at half-hourly time steps and for a longer period of record (2002–2015) but have not been quality controlled and thus are not included here.

3. Discussion

3.1. Example Scientific Applications of the Data Set

The long time series and distributed network of measurements lend themselves to answer many scientific questions. In addition to providing insight into summer thunderstorms [e.g., *Lundquist et al*., 2009] or diurnal cycles [e.g., *Lundquist et al*., 2005], which rely less on precise magnitudes, the rating curves developed here allow examination of how water masses move through different sections of the watershed at different times of year and during different types of water years. For example, Figure 2 illustrates half-hourly (a and d) and daily average (b and e) streamflow for a wet year (2010) and a dry year (2014) for the Tuolumne River at Highway 120 and the two upstream river forks that contribute to it: the Lyell Fork at Twin Bridges (which

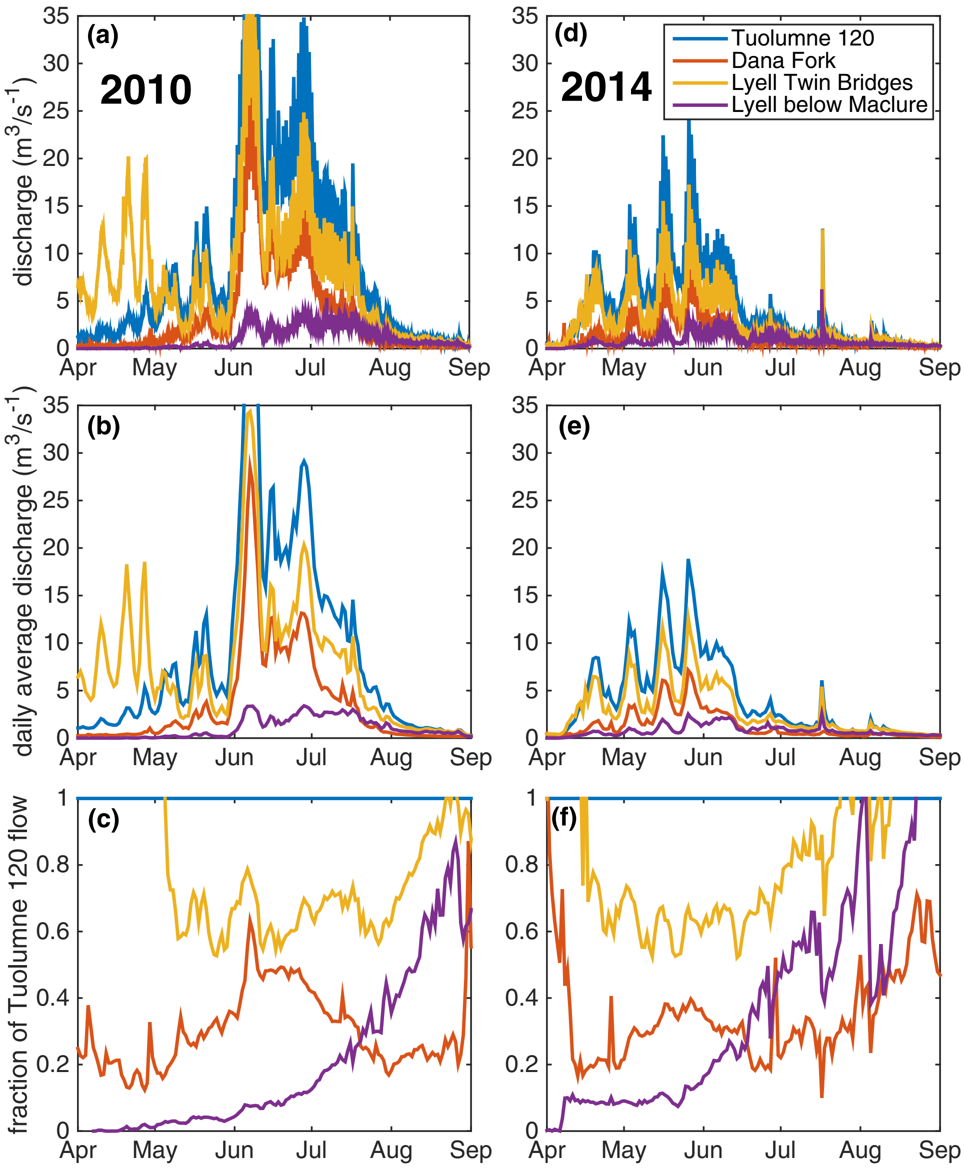

Figure 2. Illustration of dynamic discharge relationships for (a and d) half-hourly flows and (b and e) daily average flows of the Dana Fork, Lyell Fork below Maclure, Lyell Fork at Twin Bridges, and Tuolumne at 120. (c and f) Flows at the three higher sites as a fraction of daily flows at Tuolumne 120. Plots show these four subbasins in a cool-wet year (2010, a–c) and a warm-dry year (2014, d–f). By area, the Dana Fork and Lyell Fork at Twin Bridges make up about 40% and 60% of the Tuolumne at 120 drainage. The Lyell below Maclure monitors just the headwaters of the Lyell Fork, and makes up about 8% of the area contributing to Tuolumne at 120. See text for discussion.

drains about 60% of the area upstream, all granodiorite) and the Dana Fork (which drains about 40% of the area upstream, including more metamorphic and sedimentary rocks). Also shown is discharge from the Lyell Fork of the Tuolumne below Maclure Creek, which isolates just the headwaters of the Lyell Fork, draining both the Lyell and Maclure Glaciers and making up only 8% of the area contributing to the Tuolumne at Highway 120. In 2010, there were issues with ice jams in the early season, where the estimated discharge at the Lyell Twin Bridges site is higher than the estimated discharge at Tuolumne 120 just downstream. These high values are likely due to ice formations blocking water flow and causing local flooding. In both years, the early spring flows originate mainly from the Lyell Fork (with more than 60% of flows at Tuolumne 120 originating from the Lyell Fork). By the time of peak runoff, 40% or more of discharge originates from the Dana Fork, so that it is now contributing proportional to its area, if not more so. As flows decline, the relative contribution of discharge from the Dana Fork decreases, while the contribution from the Lyell Fork, particularly that originating from the glaciers above Lyell below Maclure, increases. This general pattern occurs every year. However, the timing of this trade-off, when Lyell below Maclure contributes more water than the Dana Fork, despite its smaller area, depends on the water year. In 2010 the switch occurred in mid-July (Figure 2c), while in 2014, it occurred in mid-June (Figure 2f). Summer thunderstorms temporarily decrease the relative importance of the glacier-fed Lyell below Maclure (Figures 2d–2f). Also apparent are the times when contributions from the upstream subbasins exceed 100% of flow at Tuolumne 120. This may be due to incorrect estimates for one or more of the rating curves (these differences fall within the 95%-uncertainty bounds), or may be due to streamflow infiltrating in the meadows and restoring local groundwater reserves [e.g., *Loheide and Lundquist*, 2009; *Loheide et al*., 2009].

One direct application of the data set as a whole is to test a distributed hydrological model (e.g., similar to that run by *Cristea et al*. [2014]). The Dana Meadows forcing time series could be used to run the model. The distributed temperature measurements could be used to check that the model is representing the spatial pattern of temperature correctly. The stream data could be used to check the model's representation of streamflow at multiple points within the basin. Though not provided here, the model's representation of distributed snow fields could also be compared with lidar snow depth data from the ASO program [*Painter et al*., 2016], making this a truly unique opportunity for distributed model development.

3.2. Lessons Learned From Fieldwork: Balancing Trade-Offs When Installing in a Wilderness Environment

Lessons learned from the Yosemite Hydroclimate Network may be useful to inform installations of similar hydroclimate networks in other wilderness locations. While traditional mountain precipitation gauges and snow pillows are generally quite visible, and therefore difficult to justify under the Wilderness Act, stream stage and air temperature measurements may be obtained less obtrusively. Ideally, individual installations must be robust and inexpensive, be easy to construct and install in remote regions, and need infrequent site visits. When putting a stream gauge into wilderness or other protected area where installation impacts such as visibility must be considered, one should consider (1) the time period of interest for monitoring (longer-term requires a more robust installation), (2) accessibility and feasibility of measuring high flows, (3) potential ice-jamming impacts (south-facing bedrock lined channels are more robust than meadow locations), (4) vented versus unvented pressure transducers and impacts to data quality/resolution (see Table 2), and (5) stability of the installation (see Table 2). Reference elevations, such as benchmarks, staff plates, or tapedown measurements are also critical to detect and correct for instrument movement or drift.

4. Conclusions: Uniqueness and Application

Spatially distributed measurements are needed to understand how variations in slope, aspect, elevation, soil type, vegetation, etc., influence surface processes, and these are critically important in areas of high elevations and complex terrain, such as those monitored with this data set. For example, land surface climatic feedbacks and the magnitude and timing of snowmelt runoff depend critically on the spatial heterogeneity of snow depth and melt rates [*Anderton et al*., 2002; *Blöschl and Sivapalan*, 1995; *Giorgi and Avissar*, 1997; *Liston*, 1999; *Luce et al*., 1998]. Current hydrologic models often get approximately the right answers for the wrong reasons, and model improvements can only come about through detailed checks against carefully distributed observations [*Kampf and Burges*, 2007; *Seyfried and Wilcox*, 1995]. In many cases, hydrologists still struggle to determine the dominant processes at different spatial scales, and even qualitative observations of spatial patterns can prove invaluable in analyses [*Blöschl*, 2001].

The Tuolumne watershed has been the focus in situ distributed hydrological and meteorological measurements for over 13 years, which provides a useful data set to explore distributed modeling and process representations at multiple scales.

Acknowledgments
The installation, maintenance, and quality-control of these sites and data have involved the work of many dedicated individuals. In addition to the coauthors we thank Brian Huggett, Larry Riddle, Heidi Roop, Josh Baccei, Julia Dettinger, Fred Lott, Andrey Shcherbina, Steve Loheide, Chris Lowrey, Douglas Alden, Edwin Sumargo, Reuben Demirdjian, and many more. Funding for data processing, and hence this publication, came from the National Science Foundation, CBET-0729830, and NASA Grant-NNX15AB29G. All data are currently available here, http://depts.washington.edu/mtnhydr/data/yosemite.shtml, and at CUAHSI (http://data.cuahi.org), and are permanently housed in the University of Washington Research Works Archive at http://hdl.handle.net/1773/35957. The solar radiation data time series were quality controlled using the code provided here, https://github.com/Mountain-Hydrology-Research-Group/moq, and the shortwave interpolation algorithm is available here, https://github.com/klapo/shin. We thank Jerome Le Coz for help setting up BaRatin and applying it to our sites. The code for BaRatin can be obtained by contacting Jerome Le Coz, as detailed in *Le Coz et al*. [2014].

References

Anderton, S. P., S. M. White, and B. Alvera (2002), Micro-scale spatial variability and the timing of snow melt runoff in a high mountain catchment, *J. Hydrol.*, *268*, 158–176.

Bales, R., N. Molotch, T. Painter, M. Dettinger, R. Rice, and J. Dozier (2006), Mountain hydrology of the western US, *Water Resour. Res.*, *42*, W08432, doi:10.1029/2005WR004387.

Basagic, H. J., and A. G. Fountain (2011), Quantifying 20th century glacier change in the Sierra Nevada, California, *Arct. Antarct. Alp. Res.*, *43*(3), 317–330.

Birgand, F., G. Lellouche, and T. W. Appelboom (2013), Measuring flow in non-ideal conditions for short-term projects: Uncertainties associated with the use of stage-discharge rating curves, *J. Hydrol.*, *503*, 186–195, doi:10.1016/j.jhydrol.2013.09.007.

Blöschl, G. (2001), Scaling in hydrology, *Hydrol. Processes*, *15*, 709–711.

Blöschl, G., and M. Sivapalan (1995), Scale issues in hydrological modeling: A review, *Hydrol. Processes*, *9*, 251–290.

Bohn, T. J., B. Livneh, J. W. Oyler, S. W. Running, B. Nijssen, and D. P. Lettenmaier (2013), Global evaluation of MTCLIM and related algorithms for forcing of ecological and hydrological models, *Agric. For. Meteorol.*, *176*, 38–49, doi:10.1016/j.agrformet.2013.03.003.

Burt, T. P., and J. J. McDonnell (2015), Whither field hydrology? The need for discovery science and outrageous hydrological hypotheses, *Water Resour. Res.*, *51*, 5919–5928, doi:10.1002/2014WR016839.

Coxon, G., J. Freer, I. K. Westerberg, T. Wagener, R. Woods, and P. J. Smith (2015), A novel framework for discharge uncertainty quantification applied to 500 UK gauging stations, *Water Resour. Res.*, *51*, 5531–5546, doi:10.1002/2014WR016532.

Cristea, N. C., J. D. Lundquist, S. P. Loheide, C. S. Lowry, and C. E. Moore (2014), Modelling how vegetation cover affects climate change impacts on streamflow timing and magnitude in the snowmelt-dominated upper Tuolumne Basin, Sierra Nevada, *Hydrol. Processes*, *28*, 3896–3918, doi:10.1002/hyp.9909.

Daly, C., M. Halbleib, J. I. Smith, W. P. Gibson, M. K. Doggett, G. H. Taylor, J. Curtis, and P. P. Pasteris (2008), Physiographically sensitive mapping of climatological temperature and precipitation across the conterminous United States, *Int. J. Climatol.*, *28*, 2031–2064, doi:10.1002/joc.1688.

Deardorff, J. W. (1978), Efficient prediction of ground surface temperature and moisture, with an inclusion of a layer of vegetation, *J. Geophys. Res.*, *83*(N64), 1889–1903, doi:10.1029/JC083iC04p01889.

Feld, S., N. C. Cristea, and J. D. Lundquist (2013), Representing atmospheric moisture content along mountain slopes: Examination using distributed sensors in the Sierra Nevada, California, *Water Resour. Res.*, *49*, 4424–4441, doi:10.1002/wrcr.20318.

Freeman, L. A., M. C. Carpenter, D. O. Rosenberry, J. P. Rousseau, R. Unger, and J. S. McLean (2004), Use of submersible pressure transducers in water-resources investigations. Chapter A of Book 8, Instrumentation, Section A, Instruments for measurement of water level, *Tech. of Water-Resour. Invest. 8-A3*, 65 pp. [Available at: http://pubs.usgs.gov/twri/twri8a3/.]

Giorgi, F., and R. Avissar (1997), Representation of heterogeneity effects in Earth system modeling: Experience from land surface modeling, *Rev. Geophys.*, *35*, 413–438.

Hartsough, P. C., and M. W. Meadows (2012), Critical zone observatory: Snowline processes in the Southern Sierra Nevada. *Mountain Research Initiative Newsletter No. 7, November 2012*.

Hinkelman, L., K. Lapo, N. Cristea, and J. Lundquist (2015), Using CERES SYN surface irradiance data as forcing for snowmelt simulation in complex terrain, *J. Hydrometeorol.*, *16*, 2133–2152 doi:10.1175/JHM-D-14-0179.1.

Henn, B., M. S. Raleigh, A. Fisher, and J. D. Lundquist (2013), A comparison of methods of filling gaps in near-surface air temperature data, *J. Hydrometeorol.*, *14*, 929–945, doi:10.1175/JHM-D-12-027.1.

Henn, B., M. P. Clark, D. Kavetski, and J. D. Lundquist (2015), Estimating mountain basin-mean precipitation from streamflow using Bayesian inference, *Water Resour. Res.*, *51*, 8012–8033, doi:10.1002/2014WR016736.

Huber, N. K. (1987), *The Geologic Story of Yosemite National Park*, 64 pp., U.S. Geol. Surv. Bull., *1595*, U.S. Gov. Print. Off., Washington D. C.

Hudson, R., and J. Fraser (2005), Introduction to salt dilution gauging for streamflow measurement. Part IV: The mass balance (or dry injection) method, *Streamline Watershed Manage. Bull.*, *9*(1), 6–12.

Hunsaker, C. T., T. W. Whitaker, and R. C. Bales (2012), Snowmelt runoff and water yield along elevation and temperature gradients in California's Southern Sierra Nevada, *J. Am. Water Resour. Assoc.*, *1–12*, 667–678, doi:10.1111/j.1752-1688.2012.00641.x.

Kampf, S. K., and S. J. Burges (2007), A framework for classifying and comparing distributed hillslope and catchment hydrologic models, *Water Resour. Res.*, *43*, W05423, doi:10.1029/2006WR005370.

Landry, C. C., K. A. Buck, M. S. Raleigh, and M. P. Clark (2014), Mountain system monitoring at Senator Beck basin, San Juan Mountains, Colorado: A new integrative data source to develop and evaluate models of snow and hydrologic processes, *Water Resour. Res.*, *50*, 1773–1788, doi:10.1002/2013WR013711.

Lapo, K. E., L. M. Hinkelman, C. C. Landry, A. K. Massmann, and J. D. Lundquist (2015), A simple algorithm for identifying periods of snow accumulation on a radiometer, *Water Resour. Res.*, *51*, 7820–7828 doi:10.1002/2015WR017590.

LeCoz, J., B. Renard, L. Bonnifait, F. Branger, and R. Le Boursicaud (2014), Combining hydraulic knowledge and uncertain gaugings in the estimation of hydrometric rating curves: A Bayesian approach, *J. Hydrol.*, *509*, 573–587, doi:10.1016/j.jhydrol.2013.11.016.

Liston, G. E. (1999), Interrelationships among snow distribution, snowmelt, and snow cover depletion, implications for atmospheric, hydrologic and ecologic modeling, *J. Appl. Meteorol.*, *38*, 1474–1487.

Loheide, S. P., II, and J. D. Lundquist (2009), Snowmelt-induced diel fluxes through the hyporheic zone, *Water Resour. Res.*, *45*, W07404, doi:10.1029/2008WR007329.

Loheide, S. P., II, R. S. Deitchman, D. J. Cooper, E. C. Wolf, C. T. Hammersmark, and J. D. Lundquist (2009), Hydroecology of impacted wet meadows in the Sierra Nevada and Cascade Ranges, CA, *Hydrogeol. J.*, *17*, 229–246, doi:10.1007/s10040-008-0380-4.

Lowry, C., J. Deems, S. Loheide II, and J. D. Lundquist (2010), Linking snowmelt derived recharge and groundwater flow in a high elevation meadow system, Sierra Nevada Mountains, California. *Hydrol. Processes*, *24*, 2821–2833.

Lowry, C. S., S. P. Loheide, C. Moore, J. D. Lundquist (2011), Groundwater controls on vegetation composition and patterning in mountain meadows, *Water Resour. Res.*, *47*, W00J11, doi:10.1029/2010WR010086.

Luce, C. H., D. G. Tarboton, and K. R. Cooley (1998), The influence of the spatial distribution of snow on basin-averaged snowmelt, *Hydrol. Processes*, *12*, 1671–1683.

Lundquist, J. D., and M. D. Dettinger (2005), How snowpack heterogeneity affects diurnal streamflow timing, *Water Resour. Res.*, *41*, W05007, doi:10.1029/2004WR003649.

Lundquist, J. D., and A. Flint (2006), Onset of snowmelt and streamflow in 2004 in the Western United States: How shading may affect spring streamflow timing in a warmer world, *J. Hydrometeorol.*, *7*, 1199–1217.

Lundquist, J. D., and D. R. Cayan (2007), Surface temperature patterns in complex terrain: Daily variations and long-term change in the central Sierra Nevada, California, *J. Geophys. Res.*, *112*, D11124, doi:10.1029/2006JD007561.

Lundquist, J. D., and B. Huggett (2008), Evergreen trees as inexpensive radiation shields for temperature sensors, *Water Resour. Res.*, special issue on Measurement Methods, *44*, W00D04, doi:10.1029/2008WR006979.

Lundquist, J. D., and J. Roche (2009), Climate change and water supply in western national parks, *Park Sci.*, *26*(1), 31–33.

Lundquist, J. D., D. R. Cayan, and M. D. Dettinger (2003), Meteorology and hydrology in Yosemite National Park: A sensor network application, in *Information Processing in Sensor Networks: Second International Workshop, IPSN 2003*, edited by F. Zhao and L. Guibas, pp. 518–528, Springer, N. Y.

Lundquist, J. D., D. R. Cayan, and M. D. Dettinger (2004), Spring onset in the Sierra Nevada: When is snowmelt independent of elevation?, *J. Hydrometeorol.*, *5*, 325–340.

Lundquist, J. D., M. Dettinger, and D. Cayan (2005), Snow-fed streamflow timing at different basin scales: Case study of the Tuolumne River above Hetch Hetchy, Yosemite, California, *Water Resour. Res.*, *41*, W07005, doi:10.1029/2004WR003933.

Lundquist, J. D., N. Pepin, and C. Rochford (2008), Automated algorithm for mapping regions of cold-air pooling in complex terrain, *J. Geophys. Res.*, *113*, D22107, doi:10.1029/2008JD009879.

Lundquist, J. D., B. Huggett, H. Roop, and N. Low, (2009), Use of spatially-distributed stream stage recorder to augment rain gages by identifying locations of thunderstorm precipitation and distinguishing rain from snow, *Water Resour. Res.*, *45*, W00D25, doi:10.1029/2008WR006995.

Lundquist, J. D., N. E. Wayand, A. Massmann, M. P. Clark, F. Lott, and N. C. Cristea (2015), Diagnosis of insidious data disasters, *Water Resour. Res.*, *51*, 2498–2514, doi:10.1002/2014WR016585.

Moore, C. E., S. P. Loheide, C. S. Lowry, and J. D. Lundquist (2014), Instream restoration to improve the ecohydrologic function of a subalpine meadow: Pre-implementation modeling with HEC_RAS, *J. Am. Water Resour. Assoc.*, *50*(4), 1033–1050, doi:10.1111/jawr.12155.

Moore, R. D. (2004a), Introduction to salt dilution gauging for streamflow measurement. Part 1, *Streamline Watershed Manage. Bull.*, *7*(4), 20–23.

Moore, R. D. (2004b), Introduction to salt dilution gauging for streamflow measurement. Part 2: Constant-rate injection, *Streamline Watershed Manage. Bull.*, *8*(1), 11–15.

Moore, R. D. (2005), Introduction to salt dilution gauging for streamflow measurement. Part 3: Slug injection, *Streamline Watershed Manage. Bull.*, *8*(2), 1–6.

Muir, J. (1911), *My First Summer in the Sierra*, Norman S. Berg, Dunwoody, Ga.

Natural Resources Conservation Service (2006), *Soil Survey Geographic (SSURGO) Database for Yosemite National Park, California, ca790*, U.S. Dep. of Agric., Washington, D. C. [Available at http://SoilDataMart.nrcs.usda.gov.]

Oberg, K., and D. S. Mueller (2007), Validation of streamflow measurements made with acoustic Doppler current profilers, *J. Hydraulic Eng. ASCE*, *133*, 1421–1432.

O'Neill, E. S. (1984), *Meadow in the Sky: A History of Yosemite's Tuolumne Meadows Region*, 179 pp. Albicaulis Press, Groveland, Calif.

Painter, T. H., et al. (2016), The Airborne Snow Observatory: Fusion of scanning lidar, imaging spectrometer, and physically-based modeling for mapping snow water equivalent and snow albedo, *Remote Sens. Environ.*, *184*, 139–152, doi:10.1016/jrse.2016.06.018.

Prata, A. J. (1996), A new long-wave formula for estimating downward clear-sky radiation at the surface, *Q. J. R. Meteorol. Soc.*, *122*(533), 1127–1151, doi:10.1002/qj.49712253306.

Raleigh, M. S., K. Rittger, C. E. Moore, B. Henn, J. A. Lutz, and J. D. Lundquist (2013). Ground-based testing of MODIS fractional snow cover in subalpine meadows and forests of the Sierra Nevada, *Remote Sens. Environ.*, *128*, 44–57.

Rantz, S. E. et al. (1982a), Measurement and computation of streamflow, Measurement of stage and discharge, vol. 1, *U.S. Geol. Surv. Water Supply Pap. 2175*, 284 pp., U.S. Gov. Print. Off., Washington, D. C.

Rantz, S. E., et al. (1982b), Measurement and computation of streamflow, Computation of discharge, vol. 2, *U.S. Geol. Surv. Water Supply Pap. 2175*, pp. 285–631, U.S. Gov. Print. Off., Washington, D. C.

Reba, M. L., D. Marks, M. Seyfried, A. Winstral, M. Kumar, and G. Flerchinger (2011), A long-term data set for hydrologic modeling in a snow-dominated mountain catchment, *Water Resources Res.*, *47*, W07702, doi:10.1029/2010WR010030.

Rice, R., R. C. Bales, T. H. Painter, and J. Dozier (2011), Snow water equivalent along elevation gradients in the Merced and Tuolumne River basins of the Sierra Nevada, *Water Resour. Res.*, *47*, W08515, doi:10.1029/2010WR009278.

Rittger, K., T. H. Painter, and J. Dozier (2013), Assessment of methods for mapping snow cover from MODIS, *Adv. Water Resour.*, *51*, 367–380, doi:10.1016/j.advwatres.2012.03.002.

Rittger, K., E. H. Bair, A. Kahl, and J. Dozier (2016), Spatial estimates of snow water equivalent from reconstruction, *Adv. Water Resour.*, *94*, 345–363, doi:10.1016/j.advwatres.2016.05.015.

Seyfried, M. S., and B. P. Wilcox (1995), Scale and the nature of spatial variability: Field examples having implications for hydrologic modeling, *Water Resour. Res.*, *31*(1), 173–184.